Int. J. Heat Mass Transfer. Vol. 36, No. 7, pp. 1913–1922, 1993
Printed in Great Britain

0017–9310/93 $6.00 + 0.00
Pergamon Press Ltd

Solution of Navier–Stokes equations on non-staggered grid

A. W. DATE
Mechanical Engineering Department, Indian Institute of Technology, Powai, Bombay 400 076, India

(*Received* 12 *February* 1992)

Abstract—When Navier–Stokes equations are solved on a non-staggered grid, the problem of checker board prediction of pressure is encountered. Over the last ten years, this problem has been cured by what is known as the momentum interpolation formula which is applied for evaluation of the cell-face velocities. In this paper two contributions are made. Firstly, it is shown that the momentum interpolation formula is a special case of a more general interpolation relationship that can be derived from a physical principle. In this sense, the relationship does not provide a unique formula for the interpolation of the cell-face velocity. In order to achieve unique interpolation practice, the second contribution of this paper relates to pressure-gradient interpolation. The results obtained from pressure-gradient interpolation compare extremely favourably with those obtained using staggered grid.

1. INTRODUCTION

1.1. *The problem considered*

THE SOLUTION of Navier–Stokes equations by 'control-volume' based finite-difference methods requires that the velocities that are used to satisfy the continuity equation (from which the pressure-distribution is determined) should also simultaneously satisfy the momentum equations. When this requirement is explicitly implemented, there results the now well-known staggered grid arrangement (Fig. 1(a)) in which the velocities are stored at the cell-faces, whereas the pressures (and other scalars) are stored at the cell-centres or the main grid nodes.

In the computation of three-dimensional flows in complex geometries using curvilinear body-fitted grids, several practical advantages are achieved by employing a 'non-staggered' grid arrangement (Fig. 1(b)), in which the velocities and the pressure are stored at the same location, that is, at the grid node. Though practically attractive, the arrangement is beset with one major difficulty. Thus when (a) the cell-face velocities are linearly interpolated between neighbouring nodal velocities, and (b) the pressure-gradient appearing in the nodal momentum equations is represented by straightforward central-difference approximation, the predicted pressure distribution shows checkerboard or zig-zag variation [1], whereas the predicted velocities are often nearly accurate. This difficulty is of course associated with the extent of coarseness of the grid. The finer the mesh size, the smoother is the predicted pressure distribution.

The cure for the checkerboard prediction of pressure was first proposed by Rhie and Chow [2], in which the cell-face velocities are interpolated via what is called the momentum interpolation practice rather than being linearly interpolated as mentioned in (a) above. The pressure-gradient term, of course, is evaluated as in (b) above. This practice has been followed by several investigators over the last ten years (see, for example, refs. [3–6]). There are, however, some inelegant aspects to this method, and are described in Date [7].

1.2. *The present contribution*

The purpose of this paper is two-fold:

(i) To provide a physical basis to the cell-face velocity interpolation, and hence to demonstrate that effective interpolation can in fact be achieved by a

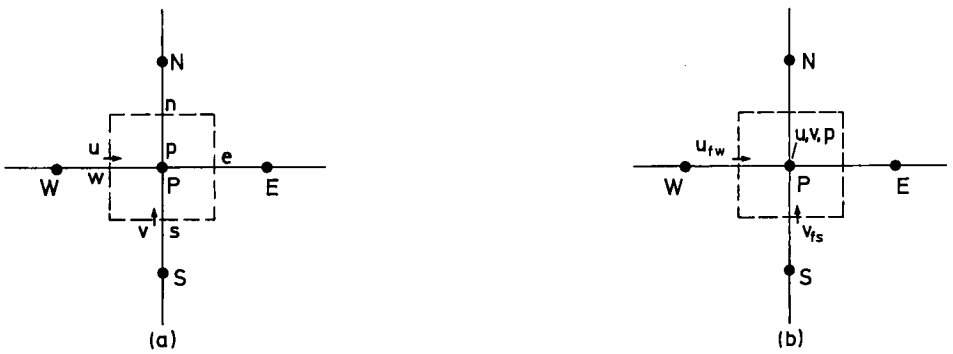

FIG. 1. Staggered (a) and non-staggered (b) grid arrangement.

NOMENCLATURE

AP, AE, AW, AN, AS	coefficients in the finite-difference equation
p	pressure
u	x-direction velocity
v	y-direction velocity
S	source term in the finite difference equation
T	temperature.

Greek symbols

β	weighting factor
μ	viscosity
ρ	density
ϕ	general variable.

Suffixes

c	correction velocity
eff	effective value
n, s, e, w	cell-face locations
P, N, S, E, W	grid node locations
f	refers to cell-face
m	arithmetic mean value
x	x-direction
y	y-direction.

Acronym

RHS	right-hand side.

much simpler formula than the one proposed by Rhie and Chow [2].

(ii) To demonstrate that the problem of checkerboard prediction of pressure can also be eliminated by interpolating the pressure-gradient in the nodal momentum equations, while still evaluating the cell-face velocities by linear interpolation.

The second contribution, it will be shown, is more attractive than the first one.

2. CELL-FACE VELOCITY INTERPOLATION

2.1. *The problem*

In this method, the nodal velocities (u, v) are distinguished from the cell-face velocities (u_f, v_f), so much so that, for greater clarity, one may write the Navier–Stokes equations as:†

$$\left(\frac{\partial u_f}{\partial x}+\frac{\partial v_f}{\partial y}\right)=0 \tag{1}$$

$$\rho\left[\frac{\partial(u_f u)}{\partial x}+\frac{\partial(v_f u)}{\partial y}\right]=-\frac{\partial p}{\partial x}+\mu\left[\frac{\partial^2 u}{\partial x^2}+\frac{\partial^2 u}{\partial y^2}\right] \tag{2}$$

$$\rho\left[\frac{\partial(u_f v)}{\partial x}+\frac{\partial(v_f v)}{\partial y}\right]=-\frac{\partial p}{\partial y}+\mu\left[\frac{\partial^2 v}{\partial x^2}+\frac{\partial^2 v}{\partial y^2}\right]. \tag{3}$$

The above equation set has three equations, but five unknowns (u_f, v_f, u, v, and p). In order to 'close' the mathematical problem, relationships of the following form are required:

$$u_f = F_u(u, v, p), \tag{4}$$

$$v_f = F_v(u, v, p), \tag{5}$$

where F_u and F_v represent the required interpolation formulae.

Equations (1)–(3) are converted into a set of linear algebraic equations by control-volume based finite-differencing. The linear set can be written in a generalized form as:

$$AP_P\phi_P = AE_P\phi_E + AW_P\phi_W + AN_P\phi_N + AS_P\phi_S + S_\phi, \tag{6}$$

where

$$AE_P = \frac{\mu}{\Delta x}-\frac{\rho u_{f_e}\Delta y}{2}$$

$$AW_P = \frac{\mu}{\Delta x}+\frac{\rho u_{f_w}\Delta y}{2}$$

$$AN_P = \frac{\mu}{\Delta y}-\frac{\rho v_{f_n}\Delta x}{2}$$

$$AS_P = \frac{\mu}{\Delta y}+\frac{\rho v_{f_s}\Delta x}{2} \tag{7}‡$$

and

$$AP_P = AE_P + AW_P + AN_P + AS_P. \tag{8}$$

The source terms S_ϕ for each ϕ are given in Table 1 below:

Table 1. S_ϕ in equation (6)

Equation	ϕ	S_ϕ
(1)	1	0
(2)	u	$(p_w-p_e)\Delta y$
(3)	v	$(p_s-p_n)\Delta x$

For uniform grid-spacing, the cell-face pressures are written as:

$$p_w = 0.5(p_W+p_P), \quad p_e = 0.5(p_E+p_P)$$

$$p_s = 0.5(p_S+p_P), \quad p_n = 0.5(p_N+p_P). \tag{9}§$$

The above practice removes appearance of p_P in the

† For the purposes of discussion, throughout this paper, the Navier–Stokes equations are written for a two-dimensional steady flow with uniform properties and without body forces.

‡ To preserve clarity in the discussion, coefficients pertaining to central-difference form are given. Also grid spacings Δx and Δy are assumed to be uniform.

§ Evaluation of pressures at the domain boundaries require special treatment as described in the Appendix.

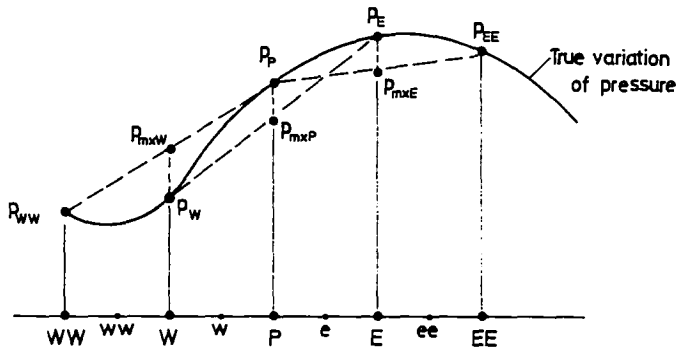

FIG. 2. The physical basis of cell-face velocity interpolation.

finite-difference equations for u_P and v_P. This is called the velocity–pressure decoupling.

The coupling between u_P, v_P, and p_P, however, can be restored by writing,

$$u_{fw} = u_{mw} = 0.5(u_W + u_P) \tag{10a}$$

$$u_{fe} = u_{me} = 0.5(u_E + u_P) \tag{10b}$$

$$v_{fs} = v_{ms} = 0.5(v_S + v_P) \tag{11a}$$

and

$$v_{fn} = v_{mn} = 0.5(v_N + v_P), \tag{11b}$$

where the suffix 'm' denotes mean values between neighbouring nodal values.

Now, since finite-difference equations for u_W, u_E, v_S and v_N will contain p_P, coupling between u_P, v_P and p_P is established. Experience, however, has shown that this coupling is very weak and in fact results in zig-zag variation of pressure [1], while the predicted velocities are often nearly accurate.

Equations (10) and (11) represent the cell-face velocities by linear interpolation and are the simplest forms of equations (4) and (5). They do not contain pressure p in an explicit manner.

2.2. *The cure*

It is possible to represent the cell-face velocity as comprising of two parts; a mean part and a correction part, so that

$$u_{fe} = u_{me} + u_{ce} \tag{12a}$$

$$u_{fw} = u_{mw} + u_{cw} \tag{12b}$$

$$v_{fn} = v_{mn} + v_{cn} \tag{13a}$$

$$v_{fs} = v_{ms} + v_{cs}; \tag{13b}$$

where suffix 'c' denotes the correction part.

Now, to evaluate the correction part, Date [7] has postulated two rules:

rule (i): the correction velocities represent the effect of 'departure from linearity' of pressure;
rule (ii): the mean velocities correspond to the linear variation of pressure.

In order to understand the application of these rules, consider Fig. 2 and concentrate attention on the w-face. The exact finite difference equation for u_{fw} then is:

$$u_{fw} = \frac{\Sigma A_k u_k|_w}{AP_w} + \frac{\Delta y}{AP_w}(p_W - p_P). \tag{14}$$

Now, rule (ii) will be applied in two ways. In the first (denoted by suffix 1), departure from linearity of pressure at P will be considered. Then,

$$u_{mw1} = \frac{\Sigma A_k u_k|_w}{AP_w} + \frac{\Delta y}{AP_w}(p_W - p_{mxP}). \tag{15}$$

In the second evaluation (denoted by suffix 2) departure from linearity of pressure at W will be considered. Then:

$$u_{mw2} = \frac{\Sigma A_k u_k|_w}{AP_w} + \frac{\Delta y}{AP_w}(p_{mxW} - p_P). \tag{16}$$

Subtraction of (15) and (16) from (14) gives:

$$u_{fw} - u_{mw1} = \frac{\Delta y}{AP_w}(p_{mxP} - p_P), \tag{17a}$$

and

$$u_{fw} - u_{mw2} = \frac{\Delta y}{AP_w}(p_W - p_{mxW}), \tag{17b}$$

where

$$p_{mxP} = 0.5(p_W + p_E) \tag{18a}\dagger$$

and

$$p_{mxW} = 0.5(p_{WW} + p_P). \tag{18b}$$

One may now require that:

$$u_{cw} = u_{fw} - u_{mw} = \beta(u_{fw} - u_{mw1}) + (1-\beta)(u_{fw} - u_{mw2}); \tag{19}$$

where β can normally be expected to take a value between 0 and 1. If $\beta = 0.5$ is chosen‡ then:

† p_{mxP} refers to mean pressure at P in x-direction. p_{myP} is given by 0.5 $(p_S + p_N)$.

‡ At present, there appears to be no independent means of determining β.

$$u_{cw} = u_{fw} - u_{mw}$$

$$= 0.5\frac{\Delta y}{AP_w}[(p_W - p_{mxW}) + (p_{mxP} - p_P)]. \quad (20)$$

Substituting for P_{mxP} and P_{mxW}, and after rearrangement,

$$u_{cw} = u_{fw} - u_{mw} = \frac{\Delta y}{AP_w}[(p_W - p_P) - 0.5(p_w - p_e) - 0.5(p_{ww} - p_w)]. \quad (20a)$$

Three comments are now pertinent:

(i) Equation (20a) confirms rule (i); if the pressure variation were to be linear, then u_{cw} will indeed be zero. u_{cw} will also tend to zero when $(\Delta x, \Delta y) \to 0$, since this further augments the AP-coefficient.

(ii) Equation (20a) is the formula proposed by Rhie and Chow [2] which is known as the momentum interpolation formula. It corresponds to $\beta = 0.5$.

(iii) Date [7] has shown that if a slight mathematical inconsistency is introduced in equations (15) and (16), then with $\beta = 0.5$, the resulting formula is the same as that used by [3–5].

Formulae for u_{ce}, v_{cs} and v_{cn} can be derived in the same manner. Thus, an expression for u_{ce}, for example, will be:

$$u_{ce} = u_{fe} - u_{me} = \frac{0.5\Delta y}{AP_e}[(p_E - p_{mxE}) + (p_{mxP} - p_P)], \quad (21)$$

where

$$p_{mxE} = 0.5(p_P + p_{EE}). \quad (22)$$

The formulae derived obey the consistency constraint. It will be shown in Section 4 that smooth variation of pressure are predicted for any value of β. The formula with $\beta = 1.0$ or $\beta = 0$ is much simpler than the momentum interpolation formula normally used.

2.3. *Some further comments*

(i) The cell-face velocity interpolation does not result in a unique formula since β can take arbitrary values. In fact, [6] represents cell-face velocities as:

$$u_f = u_m + c_1 u_c \quad (23a)$$

$$v_f = v_m + c_1 v_c \quad (23b)$$

where in the particular problem considered by him, c_1 was chosen between 0.1 and 0.5 with $\beta = 0.5$. In the present derivation, c_1 is taken as unity.

(ii) Since u_c and v_c form a part of the convective coefficient (see equation (7)) with the effect of damping oscillations in the predicted pressure, they are often described as artificial viscosity or damping terms. Note, however, that u_c and v_c can be both positive or negative.

(iii) With $c_1 = 1$, it is tempting to substitute equation (23) in equations (1)–(3). Equation (2), for example, can then be represented as:

$$\rho\left[\frac{\partial(u_m u)}{\partial x} + \frac{\partial(v_m u)}{\partial y}\right] = -\frac{\partial p}{\partial x} + \mu\left[\frac{\partial^2 u}{\partial x^2} + \frac{\partial^2 u}{\partial y^2}\right] - \rho\left[\frac{\partial(u_c u)}{\partial x} + \frac{\partial(v_c u)}{\partial y}\right]. \quad (24)$$

Now, if both equations (2) and (24) are finite-differenced by upwind differencing, the resulting forms will not be the same since,

$$|u_f| \neq |u_m| + |u_c|. \quad (25)$$

Thus, although finite-difference forms of equation (24) also yield smooth prediction of pressure, this further contributes to the non-uniqueness of the cell-face velocity interpolation.

(iv) Momentum equations written in the form of equation (24) can also be viewed as an effective pressure-gradient method in which the convecting velocities are arithmatic mean velocities and source terms are:

$$-\left.\frac{\partial p}{\partial x}\right|_{\text{eff}} = -\frac{\partial p}{\partial x} - \rho\left[\frac{\partial(u_c u)}{\partial x} + \frac{\partial(v_c u)}{\partial y}\right]. \quad (26)$$

A unique representation of the effective pressure-gradient, however, is possible as will be shown in the next section.

3. PRESSURE-GRADIENT INTERPOLATION

3.1. *Evaluation of effective pressure gradient*

On the non-staggered grids, nodal velocities (u, for example) are represented as:

$$u_P = \frac{\Sigma A_k u_k|P}{AP_P} - \frac{\Delta x \Delta y}{AP_P}\left.\frac{\partial p}{\partial x}\right|_P \quad (27)$$

$$u_W = \frac{\Sigma A_k u_k|W}{AP_W} - \frac{\Delta x \Delta y}{AP_W}\left.\frac{\partial p}{\partial x}\right|_W \quad (28)$$

and

$$u_E = \frac{\Sigma A_k u_k|E}{AP_E} - \frac{\Delta x \Delta y}{AP_E}\left.\frac{\partial p}{\partial x}\right|_E. \quad (29)$$

On the staggered grid, however, the cell-face velocities u_{fw} and u_{fe} are represented as:

$$u_{fw} = \frac{\Sigma A_k u_k|w}{AP_w} - \frac{\Delta x \Delta y}{AP_w}\left.\frac{\partial p}{\partial x}\right|_w \quad (30)$$

and

$$u_{fe} = \frac{\Sigma A_k u_k|e}{AP_e} - \frac{\Delta x \Delta y}{AP_e}\left.\frac{\partial p}{\partial x}\right|_e. \quad (31)$$

Now, on the non-staggered grids, we wish to write:

$$u_{fw} = 0.5(u_W + u_P) \quad (32)$$

$$u_{fe} = 0.5(u_E + u_P). \quad (33)$$

Substituting equations (27)–(29) in equations (32) and (33), we have:

$$u_{fw} = 0.5\left[\frac{\Sigma A_k u_k|_P}{AP_P} + \frac{\Sigma A_k u_k|_W}{AP_W}\right] - 0.5\Delta x\,\Delta y\left[\frac{1}{AP_P}\frac{\partial p}{\partial x}\bigg|_P + \frac{1}{AP_W}\frac{\partial P}{\partial x}\bigg|_W\right] \quad (34)$$

and

$$u_{fe} = 0.5\left[\frac{\Sigma A_k u_k|_P}{AP_P} + \frac{\Sigma A_k u_k|_E}{AP_E}\right] - 0.5\Delta x\,\Delta y\left[\frac{1}{AP_P}\frac{\partial p}{\partial x}\bigg|_P + \frac{1}{AP_E}\frac{\partial P}{\partial x}\bigg|_E\right]. \quad (35)$$

Comparing the pressure gradient terms in equations (34) and (35) with those in equations (30) and (31), respectively, we derive that:

$$\frac{1}{AP_w}\frac{\partial p}{\partial x}\bigg|_w \cong 0.5\left[\frac{1}{AP_P}\frac{\partial p}{\partial x}\bigg|_P + \frac{1}{AP_W}\frac{\partial p}{\partial x}\bigg|_W\right] \quad (36)$$

and

$$\frac{1}{AP_e}\frac{\partial p}{\partial x}\bigg|_e \cong 0.5\left[\frac{1}{AP_P}\frac{\partial p}{\partial x}\bigg|_P + \frac{1}{AP_E}\frac{\partial p}{\partial x}\bigg|_E\right]. \quad (37)$$

Now adding equations (36) and (37), we have:

$$\frac{1}{AP_P}\frac{\partial p}{\partial x}\bigg|_P = \frac{1}{AP_w}\frac{\partial p}{\partial x}\bigg|_w + \frac{1}{AP_e}\frac{\partial p}{\partial x}\bigg|_e - 0.5\left[\frac{1}{AP_W}\frac{\partial p}{\partial x}\bigg|_w + \frac{1}{AP_E}\frac{\partial p}{\partial x}\bigg|_E\right]. \quad (38)$$

This then represents the effective pressure gradient at nodal position P in terms of the pressure-gradients at its neighbours. This representation corresponds to the momentum satisfying cell-face velocities being represented as the arithmetic mean of the nodal velocities.

Similarly, the effective pressure gradient in the y-direction is given by:

$$\frac{1}{AP_P}\frac{\partial p}{\partial y}\bigg|_P = \frac{1}{AP_s}\frac{\partial p}{\partial y}\bigg|_s + \frac{1}{AP_n}\frac{\partial p}{\partial y}\bigg|_n - 0.5\left[\frac{1}{AP_S}\frac{\partial p}{\partial y}\bigg|_s + \frac{1}{AP_N}\frac{\partial p}{\partial y}\bigg|_N\right]. \quad (39)$$

Finally then, the finite-difference equations for u_P and v_P are represented as:

$$u_P = \frac{\Sigma A_k u_k|_P}{AP_P} - \Delta x\,\Delta y \quad [\text{RHS of equation (38)}] \quad (40)$$

and

$$v_P = \frac{\Sigma A_k v_k|_P}{AP_P} - \Delta x\,\Delta y \quad [\text{RHS of equation (39)}], \quad (41)$$

where various pressure gradients in the RHS of equations (38) and (39) are evaluated by central-differences in the usual manner, and the cell-face velocities required to calculate convective components of coefficients A_k are evaluated as mean velocities.

Finite-difference representation as above is found to remove the problem of checkerboard prediction.

3.2. *Comments on equations* (38) *and* (39)

1. If all the AP-coefficients on the RHS of equation (38) were equal and the pressure variation in the x-direction was truly linear, then the RHS of equation (38) will still equal $(P_w - P_e)/(\Delta x AP_P)$. But then for such a case, the problem of checkerboard pressure prediction does not arise [7, 8].

2. The RHS of equation (38) is not a result of a straightforward assumption of a cubic polynominal in x for

$$\frac{1}{AP}\frac{\partial p}{\partial x}\bigg|_P$$

between $x_W \leqslant x \leqslant x_E$. In fact, it is given by:

$$\text{RHS of equation (38)} = \underbrace{\frac{1}{AP_P}\frac{\partial p}{\partial x}\bigg|_P}_{\text{Term (i)}} + \frac{\Delta x^2}{4}\Bigg[\underbrace{\frac{\partial^2}{\partial x^2}\left(\frac{1}{AP}\frac{\partial p}{\partial x}\right)_P}_{\text{Term (ii)}} - 2\underbrace{\frac{\partial^2}{\partial x^2}\left(\frac{1}{AP}\frac{\partial p}{\partial x}\right)_P}_{\text{Term (iii)}}\Bigg]. \quad (42)$$

where Term (i) is evaluated by central-difference as usual, Term (ii) is evaluated by central-difference between x_e and x_w and Term (iii) is evaluated likewise between x_E and x_W.

3. Term (ii) and Term (iii) in equation (42) may thus be viewed as a correction over the usual central difference formula for $(\partial p/\partial x)|_P$. This correction becomes negligible when:

(a) $(\Delta x, \Delta y) \to 0$, since the AP coefficients are also then augmented,

(b) $\frac{1}{AP}\frac{\partial p}{\partial x}$ is constant or linear in the range $x_W < x < x_E$.

4. Equation (42) is different from equation (26), and in turn provides a unique representation of the effective pressure gradient that corresponds to the representation of the cell-face velocities as a mean of the nodal velocities.

4. RESULTS AND DISCUSSION

4.1. *Manner of presentation*

It is clear from the foregoing discussion that there are really three alternatives when Navier–Stokes equations are solved using non-staggered grid. These alternatives pertain simultaneously to:

(a) evaluation of the cell-face velocity;
(b) evaluation of the nodal pressure gradient.

The three alternatives are shown in Table 2.

The alternatives are applied to solving two one-

Table 2. Alternatives for non-staggered grid calculations

	Alt. 1	Alt. 2	Alt. 3
Pressure-gradient	Central-difference	Central-difference	By interpolation
Cell-face velocities	Linear interpolation	Complex interpolation	Linear interpolation
Remarks	1. Produces zig-zag variations of pressure unless when pressure is truly linear or when extremely fine mesh size is used	1. Removes zig-zag variation of pressure 2. Complex evaluation of cell-face velocities which must be stored. The evaluation is not unique 3. Cell-face velocities must be corrected following solution of pressure correction equation 4. The extent of agreement with the staggered grid pressure prediction depends on the value of β	1. Removes zig-zag variation of pressure 2. Simple evaluation of cell-face velocities that need not be stored 3. Cell-face velocities not corrected following solution of pressure correction equation 4. Predicted pressure variation agrees well with the staggered grid pressure distribution

dimensional problems and two two-dimensional problems. In alternative 2, two values of β are used, that is, $\beta = 1$ and 0.5; the latter value corresponds to the momentum interpolation formula of [2]. The solutions are compared with exact solutions and/or staggered grid solutions as applicable. The exact solutions are given by Date [7].

4.2. *Solution procedure*

Unlike what is described by equation (7), the coefficients in the finite-difference equations were evaluated by upwind difference. The pressure-distribution was determined by solving the pressure correction equation as described in ref. [9]. The equation was solved by using the SIMPLEC algorithm [10]. The set of finite-difference equations for all variables were solved by the Gauss–Seidel point-by-point procedure. Direct under-relaxation or false transient method were used to ensure stable convergence. Convergence was checked by the Residual Source criterion.

4.3. *One-dimensional problems*

Problem 1. *Constant mass source without momentum source.* Figure 3(a) depicts the problem considered. The exact velocity variation with x is linear, whereas the pressure variation is parabolic. Present computations were performed with 10 nodes. When Alternative 1 is used, the predicted pressure (Fig. 3(c)) shows zig-zag variation although the predicted velocity (Fig. 3(b)) is accurate. The results obtained with Alternative 2 ($\beta = 1$ and 0.5) and Alternative 3 again predict accurate velocities and the predicted pressures almost coincide with those predicted by the staggered grid solution. When the grid is refined, the solutions (not shown) with Alternative 2 and Alternative 3 were found to agree with the exact solution. With an extremely fine grid, even Alternative 1 predicted accurate pressure-distribution.

Problem 2. *Discrete momentum source without mass source.* In this problem, shown in Fig. 4(a), a momentum source of uniform strength is applied over $0.4 \leqslant x \leqslant 0.6$ (i.e. one grid node distance for 10 grid nodes computation). Thus, although the velocity is constant throughout the domain, the pressure shows discontinuous variation. Again when Alternative 1 is used, the predicted pressure variation (Fig. 4(c)) is zig-zag and in poor agreement with the exact solution. With Alternative 2, results from $\beta = 0.5$ are somewhat better than those from $\beta = 1$. Except for a minor undershoot at $x = 0.9$, results from Alternative 3 show very close agreement with the exact solution. The predicted velocities (Fig. 4(b)) are in excellent agreement with the exact solution although only 10 nodes are used. When the grid was refined, predictions with all the alternatives demonstrated close agreement with the exact solution for pressure.

4.4. *Two-dimensional problems*

Problem 1. *Square cavity problem with one moving wall.* Computations for this well-known problem were performed with a 10×10 grid.

Figure 5(a) shows the comparison of the presently predicted u-velocity profile at $x = 0.55$ with the predictions obtained with staggered grid since exact solutions are not available. The staggered grid results are interpolated between those computed at $x = 0.5$ and 0.6. The present results with all alternatives match excellently with the staggered grid results.

Differences in the predictions, however, were observed in respect of the pressure prediction (Fig. 5(b)). Results with Alternative 1 show zig-zag variation as would be expected particularly in the region where the pressure variation considerably departs from linearity. With Alternative 2, results from $\beta = 1$ are closer to the staggered grid results than from $\beta = 0.5$. Results from Alternative 3 are again close

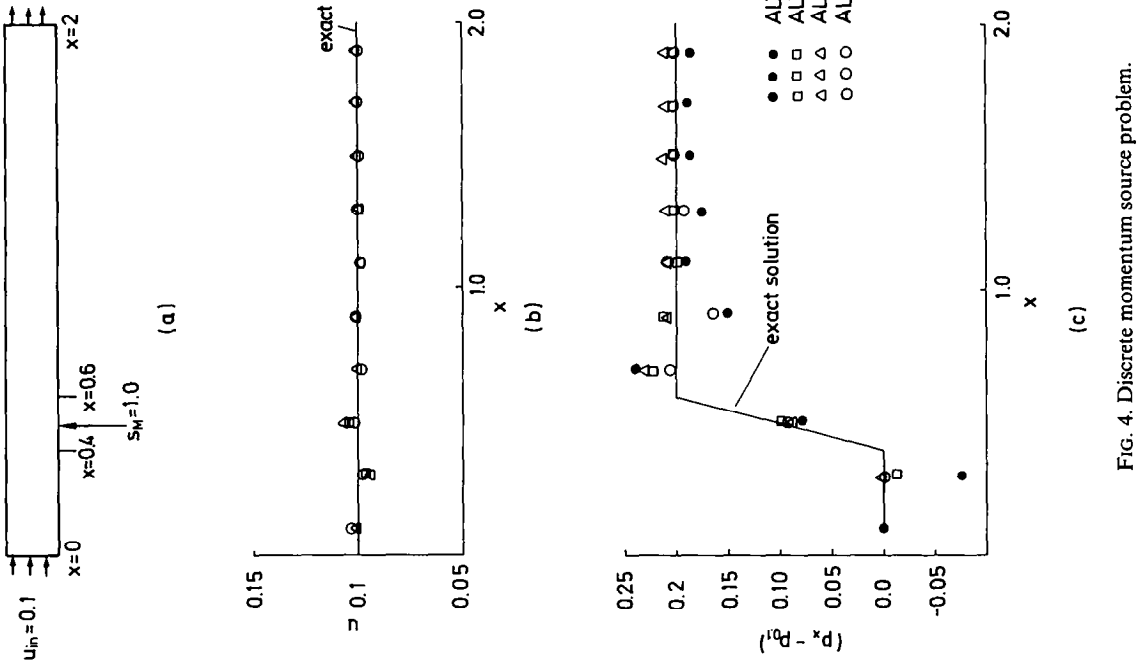

FIG. 4. Discrete momentum source problem.

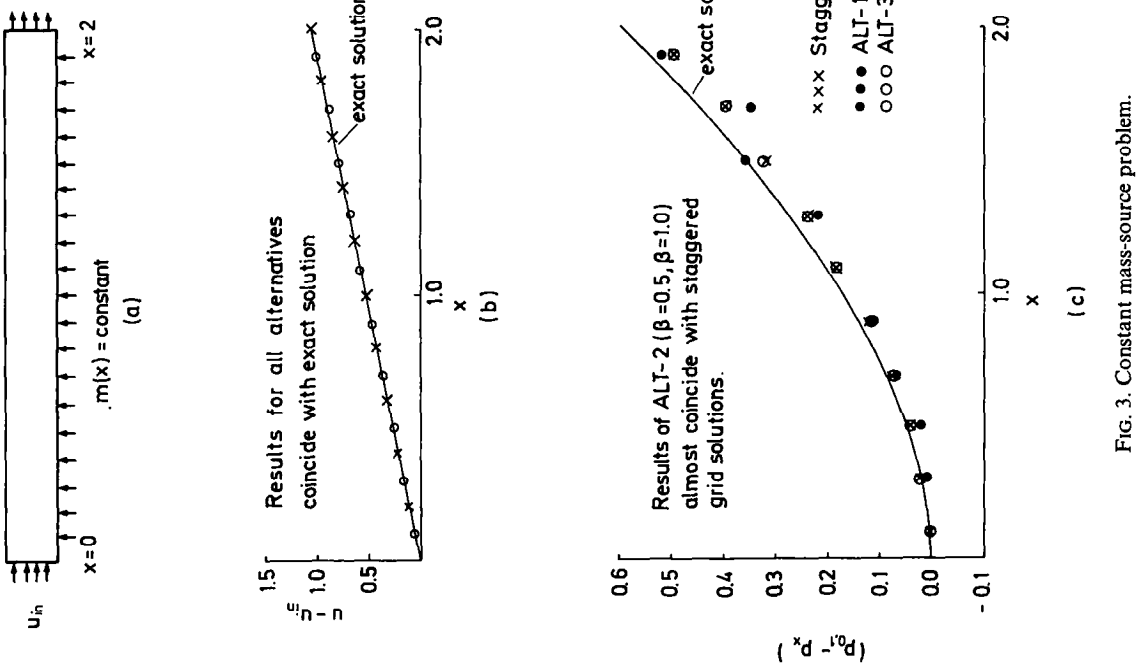

FIG. 3. Constant mass-source problem.

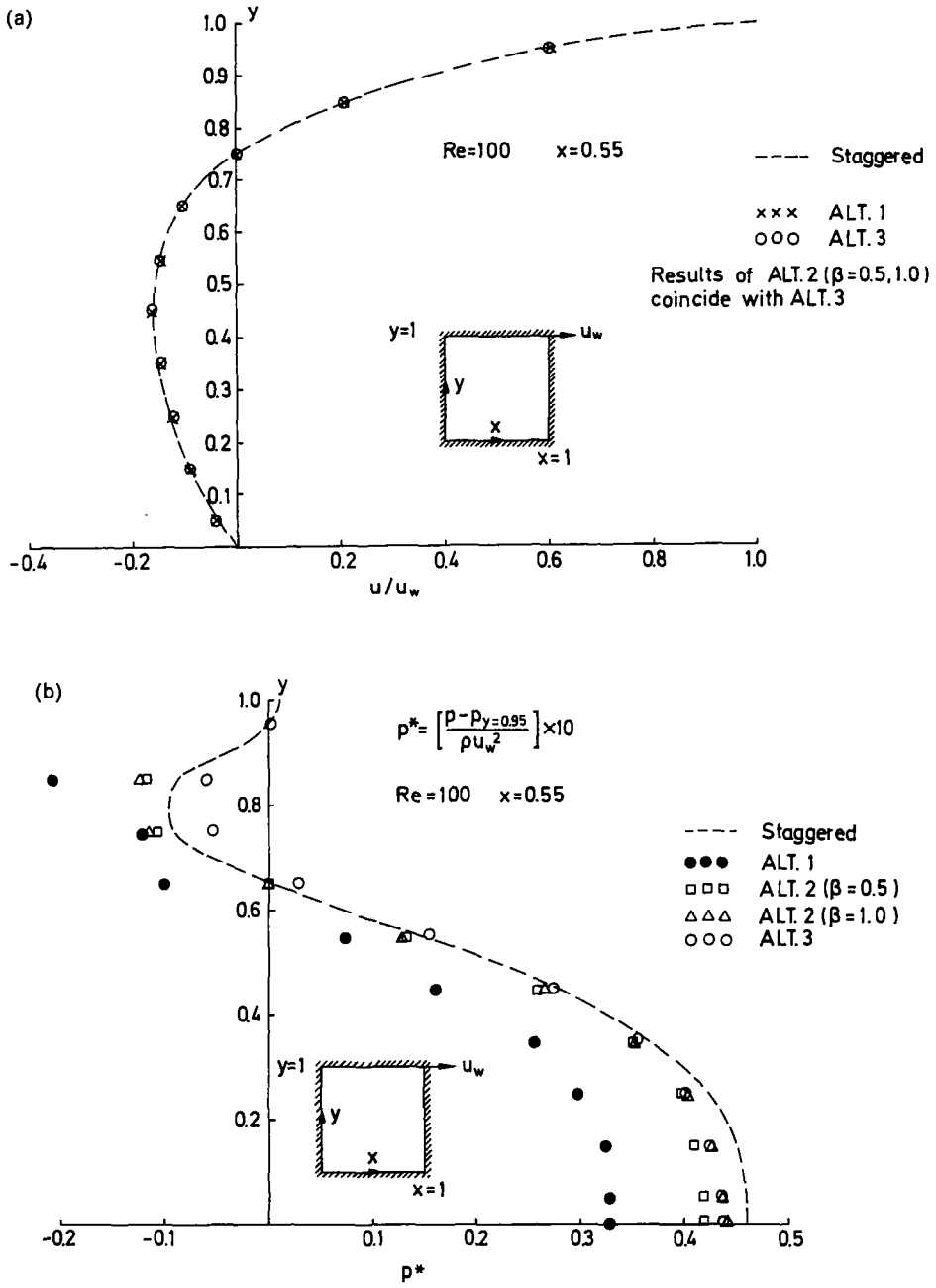

FIG. 5. (a) u/u_w at $x = 0.55$—square cavity problem. (b) Variation of pressure—square cavity problem.

to the staggered grid results. Both Alternative 2 and Alternative 3 identify the zero p^* point at $y \cong 0.65$. The agreement between staggered grid results and all the alternatives improves when the grid is refined.

Problem 2. Buoyancy-driven flow in a corner. This problem has been devised by Shih and Ren [11] and has an exact solution when the source term in the energy equation and the boundary conditions are given by prescribed algebraic relations. In this problem, equations for u, v and T are solved. At very high Rayleigh number ($Ra = 1000$ in the present case) and Prandtl numbers ($Pr = 1$ in the present case), the pressure variation in the y-direction is essentially linear and that in the x-direction is negligible. The present computations have been performed with a 10×10 grid.

Figure 6(a) shows the predicted u and v profiles at $x = 0.55$. The predictions from all alternatives match excellently with the exact solutions. The same was also found (not shown) with staggered grid computations.

Figure 6(b) shows the predicted pressure variation at $x = 0.55$. Since the exact pressure variation is essentially linear, predictions with all alternatives match excellently with the exact solution. Thus the validity of rule (ii) in Section 2.2 and that of comment (1) in Section 3.2 is confirmed.

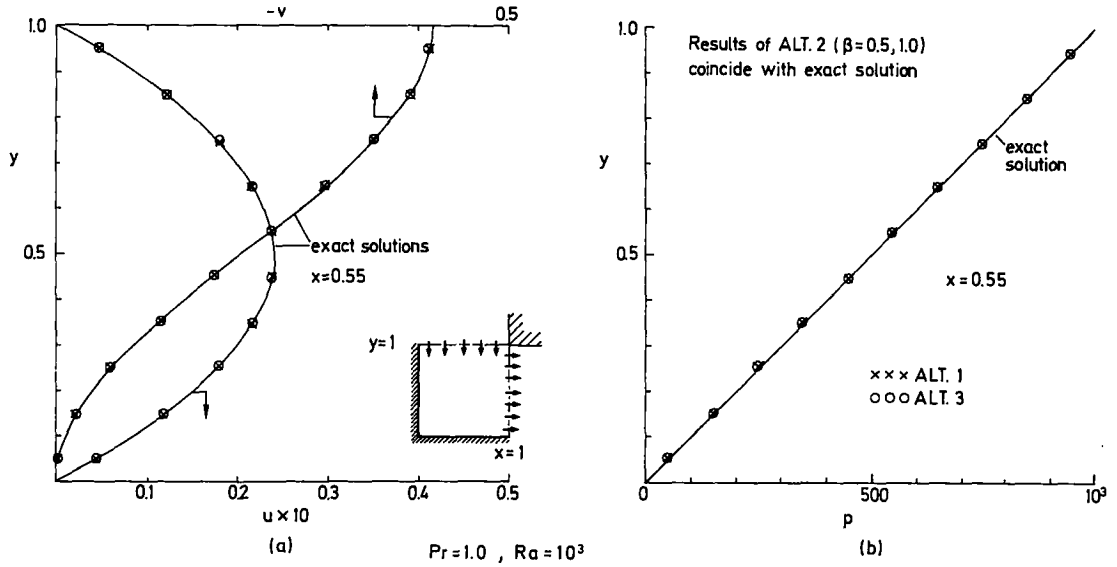

FIG. 6. Buoyancy-driven flow in a corner.

5. CONCLUSIONS

1. In this paper, it is shown that there are three alternatives to solving Navier–Stokes equations on a non-staggered grid. The relative merits of these alternatives are shown in Table 2.

2. Over the last ten years the problem of checkerboard prediction of pressure has been eliminated only by Alternative 2 with $\beta = 0.5$. In this paper it is shown that Alternative 2 does not provide unique interpolation formulae and the extent of agreement between staggered grid results and the results of this alternative depend upon the chosen value of β. In the square cavity problem, for example, $\beta = 1$ performs better than $\beta = 0.5$.

3. In this paper, Alternative 3 is newly proposed. The pressure gradient interpolation that corresponds to linear interpolation of the cell-face velocity is unique. The results from this alternative compare extremely favourably with the staggered grid results.

Acknowledgement—I am extremely grateful to Professor W. Rodi, Director, Institute for Hydromechanics, University of Karlsruhe, Germany, for enabling me to carry out this research. My grateful thanks to Dr Zhu for providing me with the relevant research papers on the subject of this research. I thank the authorities of the Indian Institute of Technology, Bombay, for giving me leave. I thank Frau Krause for her excellent typing of the manuscript.

REFERENCES

1. S. V. Patankar, *Numerical Heat Transfer and Fluid Flow*. Hemisphere, New York (1980).
2. C. M. Rhie and W. L. Chow, A numerical study of the turbulent flow past an isolated airfoil with trailing edge separation, *AIAA J.* **21**, 1525–1532 (1983).
3. M. Perić, A finite-volume method for the prediction of three-dimensional fluid flow in complex ducts, Ph.D. Thesis, University of London (1985).
4. T. F. Miller and F. W. Schmidt, Use of a pressure-weighted interpolation method for the solution of incompressible Navier–Stokes equations on a non-staggered grid system, *Numer. Heat Transfer* **14**, 213–233 (1988).
5. S. Majumdar, Development of a finite-volume procedure for prediction of fluid flow problems with complex irregular boundaries, Rep. 210/T/29, SFB 210, University of Karlsruhe, Germany (1986).
6. T. Han, Computational analysis of three-dimensional turbulent flow around a bluff body in ground proximity, *AIAA J.* **27**(2), 1213–1219 (1989).
7. A. W. Date, On interpolation of cell-face velocities in the solution of N–S equations using non-staggered grids, Rep. No. SFB 210/T/79, Sonderforschungsbereich 210, University of Karlsruhe, Germany (1991).
8. A. W. Date, Solution of N–S equations on non-staggered grids by pressure gradient interpolation, Rep. No. SFB 210/T/81, Sonderforschungsbereich 210, University of Karlsruhe, Germany (1991).
9. S. V. Patankar and D. B. Spalding, A calculation procedure for heat mass and momentum transfer in three-dimensional parabolic flows, *Int. J. Heat Mass Transfer* **15**, 1787–1806 (1972).
10. J. P. Van Doormal and G. D. Raithby, Enhancement of the SIMPLE method for predicting incompressible fluid flows, *Numer. Heat Transfer* **7**, 147–163. (1984).
11. T. M. Shih and A. L. Ren, Primitive variable formulations using non-staggered grids, *Numer. Heat Transfer* **7**, 413–428 (1984).

APPENDIX

Near-boundary node evaluation of effective pressure-gradient

With reference to Fig. A1, where the boundary at $x = 0$ is shown, the effective pressure-gradient at near boundary node P and near-near boundary node E are evaluated as:

At P:

$$\frac{1}{AP_P}\frac{\partial p}{\partial x}\bigg|_P = \frac{2}{AP_e}\frac{\partial p}{\partial x}\bigg|_e - \frac{1}{AP_E}\frac{\partial p}{\partial x}\bigg|_E. \qquad \text{(A1)}$$

At E:

Here, the RHS of equation (38) is used. Thus:

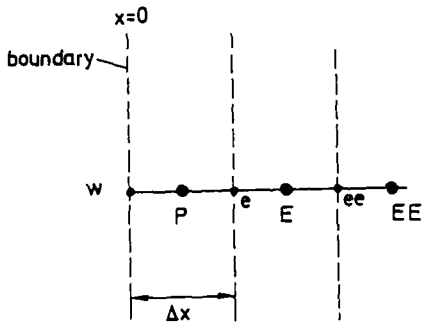

FIG. A1. Near-boundary nodes.

$$\left.\frac{1}{AP_E}\frac{\partial p}{\partial x}\right|_E = \left.\frac{1}{AP_e}\frac{\partial p}{\partial x}\right|_e + \left.\frac{1}{AP_{ee}}\frac{\partial p}{\partial x}\right|_{ee} - 0.5\left[\left.\frac{1}{AP_p}\frac{\partial p}{\partial x}\right|_P + \left.\frac{1}{AP_{EE}}\frac{\partial p}{\partial x}\right|_{EE}\right]. \quad \text{(A2)}$$

The $(\partial p/\partial x)|_P$ on the RHS of equation (A2) is evaluated as:

$$\left.\frac{\partial p}{\partial x}\right|_P = (p_E - p_w)/(3\Delta x/2) \quad \text{(A3)}$$

where

$$p_w = \left(9p_P - p_E - 3\left.\frac{\partial p}{\partial x}\right|_w \Delta x\right)\Big/8, \quad \text{(A4)}$$

or

$$\left.\frac{\partial p}{\partial x}\right|_P = \frac{1}{3}\left.\frac{\partial p}{\partial x}\right|_w + \left.\frac{\partial p}{\partial x}\right|_e - \frac{1}{3}\left.\frac{\partial p}{\partial x}\right|_E. \quad \text{(A5)}$$

In either evaluations (A2) or (A4), the value of $(\partial p/\partial x)|_w$ is provided as the boundary condition. Both evaluations provide nearly identical results.